
Advances in Computational Mathematics **16:** 157–174, 2002.

Algorithmic issues for electromagnetic scattering in layered media: Green's functions, current basis, and fast solver *

Wei Cai

Department of Mathematics, University of North Carolina at Charlotte, Charlotte, NC 28226, USA

Received 2 March 2001
Communicated by C.A. Micchelli

In this paper, we will address three computational issues for electromagnetic scattering in layered media: fast algorithm of calculating dyadic Green's functions, high order RWG current basis and fast solver for layered media. Numerical results will be included.

Keywords: electromagnetic scattering, layered media, integral equation methods, Green's functions, basis functions, fast solver

AMS subject classification: 65, 45, 78

1. Introduction

Various numerical techniques have been developed to carry out the electromagnetic field simulation, such as mode matching methods based on the eigenmode expansion of the computed object [12], finite difference time-domain (FDTD) methods with Yee scheme [43], finite element methods [33], discontinuous Galerkin methods [16,40], or integral equation methods [13,20]. The integral equation method of electromagnetic scattering of conductive surfaces is a popular approach for many applications including the parametric extraction for IC interconnects and computer packaging simulations [22], and multilayered antenna calculations [13]. The main advantage of the integral formulation [13,20] is the reduction of unknowns and the flexibility in handling complex geometry of the scatter surface. Also, the solution satisfies exterior decaying conditions by the construction of proper Green's functions in the layered medium usually encountered in those applications [18].

In applying Galerkin-type boundary element method to solve the integral equation, there are three important computational issues. The first is the calculation of the dyadic Green's function for the background medium where the scatter is embedded into, in this case, a layered medium; the second issue is the construction of appropriate current basis

* Contract/grant sponsor: National Science Foundation, Contract/grant number: CCR-9972251, CCR-9988375 and CCR-0098140.

functions; and the third one is the fast solution of the algebraic equation arising from the boundary element discretization. In this paper, we will present results in all three areas.

First, the calculation of the dyadic Green's functions in a multilayered medium has been one of the bottlenecks in the speed of integral equation methods. Extensive research has been done in the acceleration of calculation of the dyadic Green's functions in a multilayered medium [1,7,8,20]. The key difficulty is the calculation of the Sommerfeld integral appearing in the Hankel transformation, which defines the time domain dyadic Green's functions in terms of their Fourier spectral forms. Such difficulty comes from several factors:

(a) the existence of surface wave poles in the spectral forms of the Green's functions [20];

(b) the slow decay of the spectral Green's functions, especially when the field location and source location are close as the Sommerfeld integration converges extremely slow;

(c) the oscillatory behavior of the Hankel transformation kernel $J_0(z)$ and the highly oscillatory profile of the spectral Green's functions along a complex integration contour.

Several methods have been proposed to address the difficulties mentioned above. For example, the Prony-type method originally proposed in [7], later modified in [1], tries to extract the surface wave poles from the spectral form of the Green's function, then exponential functions are used to approximate the remaining part of the Green's function in the spectral domain. The main problems with this approach is the requirement of pole extraction, which has been found unstable and close to impossible when many layers of medium is considered. Also, approximation of spectral Green's functions by exponential via a Prony technique is not efficient for high frequency problem and when the source and field points are not on the same layer in a multilayered structure. Another approach [8] is trying to find a steep descent path for the Sommerfeld integration, which again is not easy for multilayered media. Recently, a new method based on window function convolution is proposed to accelerate the calculation of the Green's function for layered media [4,44]. The idea of convolution with a window function in the time domain is equivalent to a low pass filter in the frequency domain used in signal process and the Gabor transformation in wavelet theory [9]. As a result of the fast decay of the window function in the spectral domain, the window function has the same effect of a steep descent path for the Green's functions. Numerical results have confirmed the effectiveness of this method, especially, when the field and source locations are close to each other.

Secondly, to represent the current vector field over conductor's surface, it is important to have a current vector basis with continuous normal components across the interfaces among adjacent elements. The triangular RWG (Rao–Wilton–Glisson [27]) basis is a popular basis with such a property for scattering calculation. In this paper, we present a newly developed high order basis with continuous normal components [3,5], which

can be applied to either curved or flat triangular patches and/or quadrilateral patches. High order basis functions over triangular patches have been attempted in [39], however, no explicit and easy-to-implement formulations of the basis functions of general high order have been provided. Popovic and Kolundzija studied high order surface current basis functions in [25] using polynomials of parametric variables of the curved quadrilaterals and triangles with continuous normal component over generalized quadrilaterals and triangles. Later, the approach in [25] was used in [2] to produce high order of TVFE (Tangential Vector Finite Element) basis in the Sobolev space $H(Curl)$ in 2-D and 3-D spaces, similar to the edge elements proposed by Nedelec [23] and studied by others [10,41]. The method of moments (including Galerkin or collocation methods) using parametric geometry of either triangular or quadrilateral curved patches with RWG basis functions has been used in [31,34,42] for EM scattering calculations. Vector basis functions in $H(Div)$ was constructed by Raviart and Thomas for solving mixed formulation of Poisson equation [26], and later used in the calculation of eddy current in [23].

Thirdly, as the matrix equation from the Galerkin boundary element method is a full matrix, the solution of the algebraic system has been the biggest challenge in integral equation method of electromagnetic scattering problems. For most practical problems, an iterative method, such as Krylov space based GMRES method [30], has to be used. In this case, the major cost will be the product of the matrix and a solution vector, which costs $O(N^2)$ operations. In order to reduce this cost, many fast algorithms have been studied. Among them, the Fast Multipole Method (FMM) can reduce the cost to $O(N)$ or $O(N \log N)$ [11,29,38]. The FMM is based on representing the far field of the scattering wave by multipole expansions and the diagonal form of the translation operator for the Green's functions in the homogeneous medium [28]. Another method of $O(N^{4/3})$, based on Fast Steepest Descent Path Algorithm (FASDPA) representation of Hankel functions, produces a fast solver for 2-D scattering problem [19]. However, in the case of layered media, the fast solver has to be handled differently. Recently, several attempts have been made for the layered media, including the inhomogeneous plane wave expansion method using plane waves expansions of the Hankel functions [15]. Also, in [24] the FMM for free space was applied to layered media with the help of image sources. In this paper, we will propose a new fast solver based on the window acceleration calculation of Green's function for layered media and the 2-D FMM, resulting in a $O(N^{4/3} \log N)$ algorithm.

The rest of the paper is divided into the following sections: section 2, a brief introduction of the mixed potential integral equation of the electromagnetic scattering problem; section 3 gives the window function based acceleration technique; section 4 describes the high order RWG basis function. Lastly, in section 5, a fast solver is proposed for layered media.

2. Mixed potential integral equation (MPIE)

Mixed Potential Integral Equation (MPIE) is based on vector and scalar representation of the electric field [21] in terms of the current and charge variables. Integration

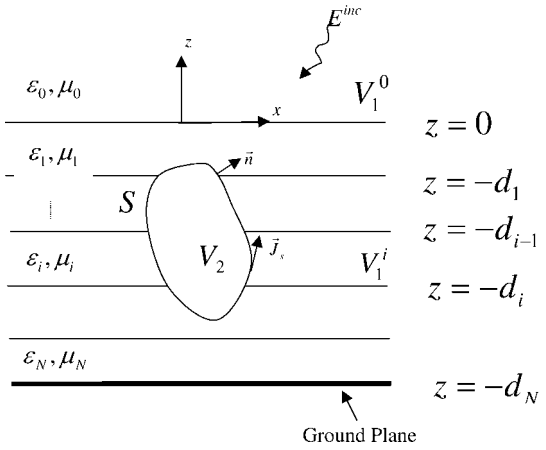

Figure 1. A scatter V_2 embedded in a multilayered medium V_1.

by parts is used to reduce the singularity of the integral equation. Such a procedure was first tried in [14].

Consider a scatterer V_2 with a surface S of an external normal $\mathbf{n}$, whose complement is denoted by V_1,embedded in a layered medium with a medium of permittivity $\varepsilon = \varepsilon(r)$ and permeability $\mu = \mu(r)$. The medium considered is shown in figure 1. It is a stratified structure consisting of $N + 1$ dielectric layers separated by N planar interfaces parallel to the $x - y$ plane of a Cartesian coordinate system and located at $z = -d_i,\ i = 0, 1, \ldots, N$.

For time harmonic fields, where the time dependence is assumed to be $\exp(j\omega t)$, the dyadic Green's function $\overline{\mathbf{G}}_E(r, r')$ satisfies the following vector wave equation,

$$\nabla \times \frac{1}{\mu(r)} \nabla \times \overline{\mathbf{G}}_E(\mathbf{r}, \mathbf{r}') - \omega^2 \varepsilon(\mathbf{r}) \overline{\mathbf{G}}_E(\mathbf{r}, \mathbf{r}') = \frac{1}{\mu(r)} \bar{\mathbf{I}} \delta(\mathbf{r} - \mathbf{r}'), \quad \mathbf{r} \in V_1. \tag{1}$$

From the Maxwell equations [6], the magnetic dyadic Green's function $\overline{\mathbf{G}}_H(r, r')$ is

$$\overline{\mathbf{G}}_H(r, r') = -\frac{1}{j\omega\mu} \nabla \times \overline{\mathbf{G}}_E(r, r'). \tag{2}$$

Also from [6], we have the following integral representation for the electromagnetic fields $\mathbf{E}_1, \mathbf{H}_1$ in V_1.

$$\mathbf{E}_1(\mathbf{r}) = \mathbf{E}^{\text{inc}}(\mathbf{r}) - \mu(\mathbf{r}) \int_{\mathbf{S}} ds' \Big[j\omega \mathbf{J}_{e(s)}(\mathbf{r}') \cdot \overline{\mathbf{G}}_E^1(\mathbf{r}', \mathbf{r}) + \frac{1}{\mu(\mathbf{r}')} \mathbf{J}_{m(s)}(\mathbf{r}') \cdot \nabla \times \overline{\mathbf{G}}_E^1(\mathbf{r}', \mathbf{r}) \Big], \quad \mathbf{r} \in V_1, \tag{3}$$

where $\overline{\mathbf{G}}_E^1(\mathbf{r}', \mathbf{r})$ is the dyadic Green's functions for the region V_1 and $\mathbf{E}^{\text{inc}}(\mathbf{r})$ is an incident field and the equivalent surface currents over S are defined as

$$\mathbf{J}_{e(s)}(\mathbf{r}) = \mathbf{n} \times \mathbf{H}_1(\mathbf{r}), \tag{4}$$

$$\mathbf{J}_{m(s)}(\mathbf{r}) = -\mathbf{n} \times \mathbf{E}_1(\mathbf{r}) \tag{5}$$

with s denoting surface currents.

For a MPIE, the electrical field is expressed in terms of a vector potential $\mathbf{A}$ and a scalar potential V_e, i.e.,

$$\mathbf{E} = -j\omega\mathbf{A} - \nabla V_e, \tag{6}$$

where

$$\nabla^2\mathbf{A} + k^2\mathbf{A} - \mu\nabla\frac{1}{\mu} \times \nabla \times \mathbf{A} = -\mu\mathbf{J}_e \tag{7}$$

and the Lorentz Gauge condition is used to relate V_e to $\mathbf{A}$, i.e.,

$$\nabla \cdot \mathbf{A} = -j\omega\varepsilon\mu V_e. \tag{8}$$

Thus, V_e satisfies the following Helmholtz equation

$$\nabla^2 V_e + k^2 V_e = -\frac{1}{\varepsilon}\rho_e, \tag{9}$$

where $k^2 = \omega^2\varepsilon\mu$ and the electric charge ρ_e is related to $\mathbf{J}_e$ by the continuity equation,

$$\rho_e = -\frac{1}{j\omega}\nabla \cdot \mathbf{J}_e. \tag{10}$$

Now assuming that the magnetic current vanishes, i.e., $\mathbf{J}_{m(s)} = 0$, and applying the impedance boundary condition [32] over S, we have

$$\mathbf{n} \times \mathbf{E}^1 = \mathbf{n} \times \left(\mathbf{E}^s + \mathbf{E}^{\text{inc}}\right) = Z_s \mathbf{n} \times \mathbf{J}_s, \tag{11}$$

where $\mathbf{J}_s = \mathbf{J}_{e(s)}$ and $\mathbf{E}^s$ is the scattered field and Z_s is the surface impedance, thus, we have the following MPIE

$$\begin{aligned} &\mathbf{n} \times j\omega\mu\left[j\omega \int_S \overline{\mathbf{G}}_A \cdot \mathbf{J}_s \, \mathrm{d}s - \nabla \cdot \int_S \frac{j\omega}{k^2}\nabla\overline{\mathbf{G}}_A \cdot \mathbf{J}_s \, \mathrm{d}s\right] \\ &\quad = \mathbf{n} \times Z_s\mathbf{J}_s - \mathbf{n} \times \mathbf{E}^{\text{inc}}, \quad \mathbf{r} \in V_1. \end{aligned} \tag{12}$$

Such a formulation reduces the degree of the singularities of the surface integration, and a Galerkin procedure will be applied to (12) where the current $\mathbf{J}_s$ and charge ρ_s are expressed in terms of N terms of high order RWG basis function, namely,

$$\mathbf{J}_s(\mathbf{r}) = \sum_{k=1}^{N} I_k \mathbf{J}_k(\mathbf{r}) \quad \text{and} \quad \rho_s(\mathbf{r}) = \sum_{k=1}^{N} I_k \rho_k(\mathbf{r}),$$

where $\rho_k(\mathbf{r}) = -(1/j\omega)\nabla \cdot \mathbf{J}_k(\mathbf{r})$.

A Galerkin projection procedure will yield the following algebraic equation

$$\sum_{l=1}^{N} Z_{kl} I_l = V_k, \quad k = 1, 2, 3, \ldots, N. \tag{13}$$

3. Fast algorithm for calculating dyadic Green's functions

As the multilayered medium in figure 1 is radial symmetric in the $(x–y)$-plane, we can apply the 2-dimensional Fourier transform to the Maxwell equations [18] to obtain the components of the dyadic Green's function in the Fourier transform (spectral) domain.

It can be shown that the Fourier transform $\widetilde{f}(k_\rho)$ of $f(\rho)$ can be written as

$$\widetilde{f}(k_\rho) = \mathcal{F}\{f(\rho)\} = S_0[f(\rho)](k_\rho) \tag{14}$$

and

$$f(\rho) = \mathcal{F}^{-1}\{\widetilde{f}(k_\rho)\} = S_0[\tilde{f}(k_\rho)](\rho), \tag{15}$$

where $\rho = \sqrt{x^2 + y^2}$, $k_\rho = \sqrt{k_x^2 + k_y^2}$, and the nth order Hankel transform $S_n[\widetilde{f}(k_\rho)]$, for integer $n \geqslant 0$, is defined as

$$S_n[\widetilde{f}(k_\rho)](\rho) = \int_0^\infty \widetilde{f}(k_\rho) J_n(k_\rho \rho) k_\rho^{n+1} \, \mathrm{d}k_\rho \tag{16}$$

and the roles of ρ and k_ρ can be switched and where $J_n(z)$ is the nth order Bessel function.

Therefore, we only have to discuss acceleration algorithms for calculating the Hankel transformation

$$G(\rho, z; z') = S_0(\widetilde{G}(k_\rho, z; z')) = \int_C \widetilde{G}(k_\rho, z; z') J_0(\rho k_\rho) k_\rho \, \mathrm{d}k_\rho, \tag{17}$$

where the contour C should be in the first quadrant of the complex wavenumber k_ρ space from 0 to ∞.

In order to accelerate the calculation of $G(\rho, z; z')$ when $z \sim z'$ or $z = z'$, we introduce the following mth order window function $\psi_a(x, y) = \psi_a(\rho)$ with a support size a,

$$\psi_a(\rho) = \begin{cases} \left(1 - \left(\dfrac{\rho}{a}\right)^2\right)^m, & \text{if } \rho \leqslant a, \\ 0, & \text{otherwise.} \end{cases} \tag{18}$$

For any cylindrical symmetrical function $f(\rho)$, we have the following identity

$$f(x, y) * \psi_a(x, y) = S_0[\widetilde{f}(k_\rho) \widetilde{\psi}_a(k_\rho)](\rho), \tag{19}$$

where

$$\widetilde{f}(k_\rho) = S_0\big[f(\rho)\big](k_\rho)$$

and

$$\widetilde{\psi}_a(k_\rho) = S_0\big[\psi_a(\rho)\big](k_\rho).$$

As a result of (19) and a Taylor expansion for the convolution term, we can approximate $f(x, y)$ as follows,

$$f(x, y) = \frac{1}{M_0} S_0\big[\widetilde{f}(k_\rho)\widetilde{\psi}_a(k_\rho)\big](\rho) + \mathrm{O}\big(a^2\big) \quad \text{as } a \to 0, \tag{20}$$

where

$$M_0 = \frac{1}{2\pi} \int_{\sqrt{x^2+y^2}\leqslant a} \psi_a(x, y)\,\mathrm{d}x\,\mathrm{d}y = \frac{a^2}{2(m+1)}.$$

Applying (20) to $G(\rho, z'; z')$, we obtain following algorithm.

Algorithm 1 (Fast algorithm for $G(\rho, z; z')$).

For $\rho > a$,

$$G\big(\rho, z; z'\big) = \frac{1}{M_0} W_0(\rho) + \mathrm{O}\big(a^2\big) \quad \text{as } a \to 0, \tag{21}$$

where

$$W_0(\rho) = S_0\big[\widetilde{G}\big(k_\rho, z; z'\big)\widetilde{\psi}_a(k_\rho)\big](\rho). \tag{22}$$

In order to get a better approximation to function $G(\rho, z'; z')$, we will rewrite $G(\rho, z'; z')$ as

$$G\big(\rho, z; z'\big) = \frac{G_2(\rho, z; z')}{r^2}, \tag{23}$$

where $r = \sqrt{x^2 + y^2 + (z - z')^2}$. From the singularity property of the vector and scalar potential Green's function [37], we can assume that $G_2(\rho, z; z') = r^2 G(\rho, z; z')$ is a smoother function, and the approximation (20) thus can be used with better accuracy.

Let $G_2(\rho, z; z') = r^2 G(\rho, z; z')$, $r = \sqrt{\rho^2 + (z - z')^2}$, then

$$G_2\big(\rho, z; z'\big) * \psi_a(x, y) = r^2 W_0(\rho) - 2\rho W_1(\rho) + W_2(\rho), \tag{24}$$

where

$$W_1(\rho) = S_1\big[\widetilde{G}\big(k_\rho, z; z'\big)\widetilde{\psi}_a^*(k_\rho)/k_\rho\big](\rho), \tag{25}$$

$$W_2(\rho) = S_0\big[\widetilde{G}\big(k_\rho, z; z'\big)\widetilde{\psi}_a^{**}(k_\rho)\big](\rho) \tag{26}$$

and

$$\widetilde{\psi}_a(k_\rho) = S_0\big[\psi_a(\rho)\big](k_\rho) = \int_0^a \psi_a(\rho) J_0(k_\rho\rho)\rho \,\mathrm{d}\rho, \tag{27}$$

$$\widetilde{\psi}_a^*(k_\rho) = S_1\big[\psi_a(\rho)\big](k_\rho) = \int_0^a \psi_a(\rho) J_1(k_\rho\rho)\rho^2 \,\mathrm{d}\rho, \tag{28}$$

$$\widetilde{\psi}_a^{**}(k_\rho) = \int_0^a \psi_a(\rho) J_0(k_\rho\rho)\rho^3 \,\mathrm{d}\rho. \tag{29}$$

Therefore, we have the following approximation scheme to the Green's function.

Algorithm 2 (Fast algorithm for $G(\rho, z; z')$).

If $\rho > 0, a \to 0$, then

$$G\big(\rho, z; z'\big) = \frac{1}{M_0 r^2}\big[r^2 W_0(\rho) - 2\rho W_1(\rho) + W_2(\rho)\big] + \mathrm{O}\big(a^2\big). \tag{30}$$

In order to calculate $W_0(\rho)$, $W_1(\rho)$ and $W_2(\rho)$ efficiently, we use the decaying property of $\widetilde{\psi}_a(k_\rho)$ and $\widetilde{\psi}_a^*(k_\rho)$ and $\widetilde{\psi}_a^{**}(k_\rho)$. It can be shown that as $|k_\rho| \to \infty$,

$$\big|\widetilde{\psi}_a(k_\rho)\big| = \mathrm{O}\big(|ak_\rho|^{-m}\big), \tag{31}$$

$$\big|\widetilde{\psi}_a^*(k_\rho)\big| = \mathrm{O}\big(|ak_\rho|^{-m+1}\big), \tag{32}$$

$$\big|\widetilde{\psi}_a^{**}(k_\rho)\big| = \mathrm{O}\big(|ak_\rho|^{-m}\big). \tag{33}$$

The fast decay condition of (31)–(33) insures that a short integration contour can be selected without sacrificing the accuracy of approximation of algorithms 1 and 2.

It is well known that the spectral form $\widetilde{G}(k_\rho, z; z')$ has surface wave poles which are located in the fourth quadrant of the complex k_ρ plane, therefore, we should deform the integration contour in the definition of $W_i(\rho)$, $i = 0, 1, 2$, to a complex contour which stays away from the surface poles. A simple contour C is suggested in figure 2

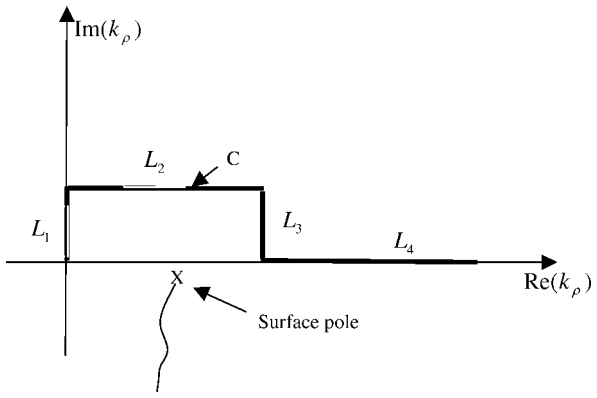

Figure 2. Contour C.

which consists of four straight segments L_i, $1 \leqslant i \leqslant 4$. The last segment L_4 will be finite and is determined by the decay properties of (31)–(33).

To maintain the second order accuracy $O(a^2)$ of algorithms 1 and 2, we choose L_4 portion of the contour C in figure 2 to satisfy the following minimum condition, while using the decay condition (31)–(33),

$$L_4 \geqslant \left[\frac{C_\infty}{a^2(m-s-3)}\right]^{1/(m-s-3)}, \tag{34}$$

where we assume that for $k_\rho \in [k_{\max}, \infty)$, we have for some integer s and constant C_∞

$$\left|\widetilde{G}(k_\rho, z; z')\right| \leqslant C_\infty (k_\rho)^s.$$

The window support a is the primary parameter to consider, which is determined by the second order accuracy estimate (30). Once a is selected, the length of the contour L_4 should be given by (34). We have found out in our numerical tests, a window $\psi_a(\rho)$ of order five ($m = 5$) is a good overall choice.

3.1. *Numerical results – $G_V(\rho, z; z')$ for a five layered medium*

In this test case, we calculate the scalar potential Green's functions $G_V(\rho, z; z')$ for a five layered medium depicted in figure 3. Four dielectric layers are used between the open air and a PEC ground plane. The relative dielectric constants for the four dielectric layers are, from top to bottom, $\varepsilon_1 = 9.6$, $\varepsilon_2 = 12.5$, $\varepsilon_1 = 2.4$, $\varepsilon_1 = 3.6$, respectively. And their corresponding thickness are $h_1 = 0.001$ m, $h_2 = 0.003$ m, $h_1 = 0.002$ m, $h_1 = 0.0015$ m, respectively.

Window $\psi_a(\rho)$ of order $m = 5$ with support size $a = 0.001$ m is used in algorithm 2 and the $L_4 = 20/a$ is the last portion of the contour C in figure 2. Figure 4 contains the magnitude and imaginary and real parts (top to bottom, lines are from integration of Hankel transform (17), symbols are results of algorithm 2) of the scalar Green's function $G_V(\rho, z; z')$ with $z = -0.0035$ m, $z' = -0.0062$ m.

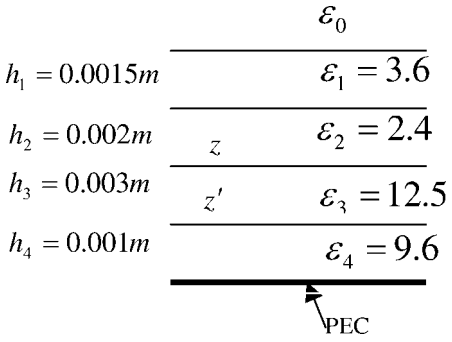

Figure 3. A 5 layered medium.

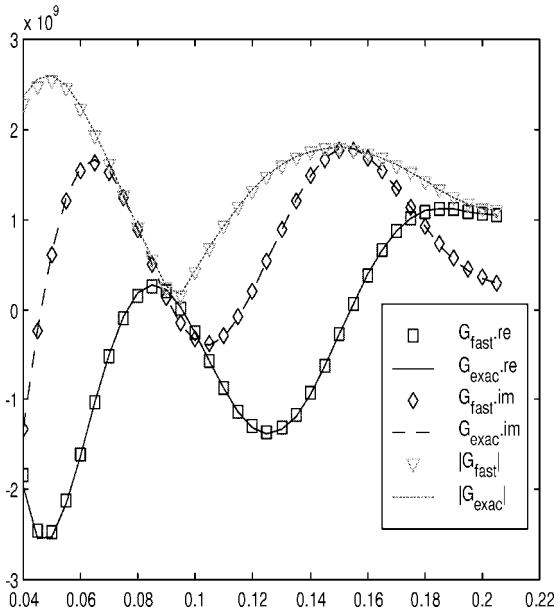

Figure 4. Scalar potential Green's function G_V (from top to bottom: the magnitude and imaginary and real parts, lines are from direct integration of Hankel transform (17), symbols are results of algorithm 2).

4. High order RWG basis functions

In a Galerkin approximation, equation (12) is multiplied by a test function $\mathbf{J}_l(\mathbf{r})$ and then, integrated over the surface S. In order to transfer the ∇ operator in the second term in (12) to the test function via integration by parts, normal continuity of $\mathbf{J}_l(\mathbf{r})$ is needed across the common interface of triangular patches. Here we present such a current basis function, the normal continuity of the current basis function is the key property of the popular RWG basis functions, which insures no accumulation of charges across the element interfaces. In the following, we will give the formulation of higher order extension of the original RWG basis over arbitrary triangular curved patches. The details of the derivation of the basis function can be found in [3,5].

Let Σ be a curved triangular surface in $\mathbb{R}^3$ and Σ is parameterized by $\mathbf{x} = \mathbf{x}(u_1, u_2),\ (u_1, u_2) \in T_0,\ T_0$ is a standard reference triangle in figure 5.

Tangential vectors: $\partial_i \mathbf{x},\ i = 1, 2$, are defined as

$$\partial_i \mathbf{x} = \frac{\partial \mathbf{x}}{\partial u_i}, \quad i = 1, 2. \tag{35}$$

Metric tensor: The distance between two points on Σ parameterized by (u_1, u_2) and $(u_1 + \mathrm{d}u_1,\ u_2 + \mathrm{d}u_2)$ is given by

$$(\mathrm{d}s)^2 = g_{\mu\nu}(u)\, \mathrm{d}u_\mu\, \mathrm{d}u_\nu, \tag{36}$$

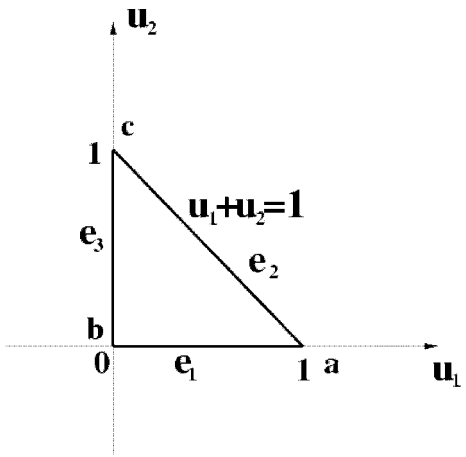

Figure 5. Reference triangle T_0.

where repeated indices imply summation

$$g_{\mu\nu} = \frac{\partial \mathbf{x}}{\partial u_\mu} \cdot \frac{\partial \mathbf{x}}{\partial u_\nu}, \quad 1 \leqslant \mu, \nu \leqslant 2, \tag{37}$$

and $\{g_{\mu\nu}\}$ is defined as the covariant tensor [17]. The determinant of $\{g_{\mu\nu}\}$ is denoted by

$$g = \det\{g_{\mu\nu}\} = g_{11}g_{22} - g_{12}^2 = \|\partial_1 \mathbf{x} \times \partial_2 \mathbf{x}\|^2. \tag{38}$$

4.1. Hierarchical polynomial basis over triangle T_0

Let T_0 be the reference triangle with vertices $a,\ b,\ c$ in figure 5, we group (u_1, u_2) polynomials into three modes: vertex modes, edge modes and internal modes [36].

– Vertex modes:

$$\begin{aligned} g_a(u_1, u_2) &= u_1, \\ g_b(u_1, u_2) &= 1 - u_1 - u_2, \\ g_c(u_1, u_2) &= u_2. \end{aligned} \tag{39}$$

Each vertex mode will take value 1 at one vertex and zero at other two vertices.

– Edge modes: for $2 \leqslant l \leqslant M$

$$\begin{aligned} g_l^{ab}(u_1, u_2) &= g_a(u_1, u_2) g_b(u_1, u_2) p_{l-2}(g_b - g_a), \\ g_l^{bc}(u_1, u_2) &= g_b(u_1, u_2) g_c(u_1, u_2) p_{l-2}(g_c - g_b), \\ g_l^{ca}(u_1, u_2) &= g_c(u_1, u_2) g_a(u_1, u_2) p_{l-2}(g_a - g_c), \end{aligned} \tag{40}$$

where $p_l(\xi),\ \xi \in [-1, 1]$ is lth order Legendre polynomial.
Each of the edge mode is only nonzero along one edge of the triangle T_0.

– Internal modes: $0 \leqslant k + l \leqslant M - 3$

$$g^{\text{int}}_{l,k}(u_1, u_2) = g_a(u_1, u_2) g_b(u_1, u_2) g_c(u_1, u_2) p_k(2g_c - 1) p_l(g_b - g_a). \tag{41}$$

And each of the internal mode will vanish over all edges of T_0.

4.2. *High order current basis functions over curved triangular patches*

Consider two curved triangular patches T^+ and T^- with a common interface AC with length ℓ in figure 6. Let T^+ and T^- be parameterized, respectively, by

$$\mathbf{x} = \mathbf{x}^+(u_1, u_2) : T_0 \to T^+, \tag{42}$$

$$\mathbf{x} = \mathbf{x}^-(u_1, u_2) : T_0 \to T^-. \tag{43}$$

We assume that the interface AC in both T^+ and T^- is parameterized by $u_1 + u_2 = 1$ and is labeled as side e_2^+ in T^+ and side e_2^- in T^-.

In [3], the following basis functions with continuous normal components are constructed.

High order basis. High order basis function for a triangular and triangular patch in figure 6 can be written as [3,5].

$$\mathbf{f}(\mathbf{x}) = \begin{cases} \dfrac{l}{\sqrt{g^+}}(P_1^+(u_1, u_2)\partial_1\mathbf{x} + P_2^+(u_1, u_2)\partial_2\mathbf{x}) & \text{if } \mathbf{x} = \mathbf{x}^+(u_1, u_2) \in T^+, \\ \dfrac{l}{\sqrt{g^-}}(P_1^-(u_1, u_2)\partial_1\mathbf{x} + P_2^-(u_1, u_2)\partial_2\mathbf{x}) & \text{if } \mathbf{x} = \mathbf{x}^-(u_1, u_2) \in T^-, \end{cases}$$

where

$$\begin{aligned} P_1^+(u_1, u_2) &= I_n^a g_A(u_1, u_2) + \sum_{m=2}^{M} \frac{I_n^{(m)} - \tilde{I}_t^{(m)}}{2} g_m^{e_2^+}(u_1, u_2) + \sum_{(l,m)\in L_\Delta} c_{lm}^1 g_{lm}^{\text{int}}, \\ P_2^+(u_1, u_2) &= I_n^c g_C(u_1, u_2) + \sum_{m=2}^{M} \frac{I_n^{(m)} + \tilde{I}_t^{(m)}}{2} g_m^{e_2^+}(u_1, u_2) + \sum_{(l,m)\in L_\Delta} c_{lm}^2 g_{lm}^{\text{int}} \end{aligned} \tag{44}$$

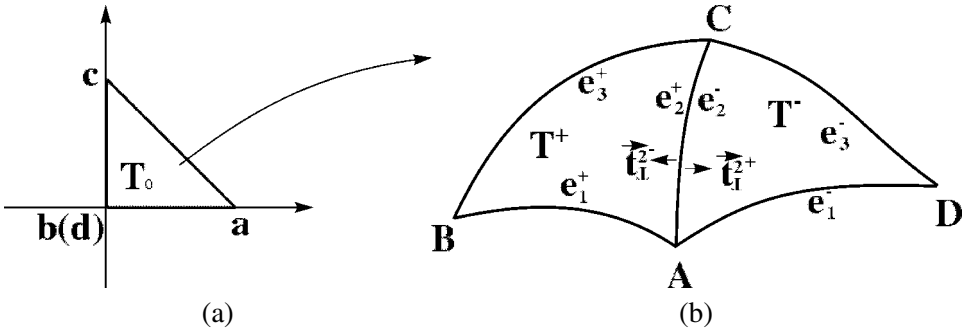

(a) (b)

Figure 6. (a) reference triangle T_0, (b) curved triangular and triangular patches.

and

$$P_1^-(u_1,u_2) = -I_n^a g_A(u_1,u_2) + \sum_{m=2}^{M} \frac{-I_n^{(m)} - \hat{I}_t^{(m)}}{2} g_m^{e_2^-}(u_1,u_2) + \sum_{(l,m)\in L_\Delta} d_{lm}^1 g_{lm}^{\text{int}},$$
$$P_2^-(u_1,u_2) = -I_n^c g_C(u_1,u_2) + \sum_{m=2}^{M} \frac{-I_n^{(m)} + \hat{I}_t^{(m)}}{2} g_m^{e_2^-}(u_1,u_2) + \sum_{(l,m)\in L_\Delta} d_{lm}^2 g_{lm}^{\text{int}} \tag{45}$$

with $e_2^+ = e_2^- = AC$,

$$\mathcal{L}_\Delta = \big\{(l,m),\ 0 \leqslant l+m \leqslant M-3\big\}. \tag{46}$$

Unknowns for each edge AC are

$$I_n^a,\ I_n^c,\ I_n^{(m)},\ \tilde{I}_t^{(m)},\ \hat{I}_t^{(m)}, \quad 2 \leqslant m \leqslant M \tag{47}$$

and interior unknowns for each triangular patch are

$$c_{lm}^1,\ c_{lm}^2,\ d_{lm}^1,\ d_{lm}^2 \quad (l,m) \in L_\Delta. \tag{48}$$

4.3. Numerical results – scattering of a 3-D sphere

As a numerical test of the high order basis function, we compute the RCS of the scattering of a 3-D perfect conducting sphere with the proposed basis functions of three different orders. Exact parametric representation of the sphere is used in the construction of the basis functions except for the original RWG basis where flat triangles are used to triangulate the sphere.

We assume that the incident wave is plane wave, i.e.,

$$\mathbf{E}^{\text{inc}}(\mathbf{r}) = E_0 \mathbf{u}_x e^{j\mathbf{k}\cdot\mathbf{r}},$$

where $\mathbf{u}_x$ is the unit vector of x-coordinate and $E_0 = 1.5$ and the propagation vector $\mathbf{k}$ is

$$\mathbf{k} = k(\sin\theta_0\cos\varphi_0, \sin\theta_0\sin\varphi_0, \cos\theta_0)$$

with $\theta_0 = 0$.

In figure 7, we show the bistatic RCS for the three methods with $N = 288$. The radius of the sphere $a = (3/\pi)\lambda$, where $\lambda = (2\pi/k)$, $k = \omega\sqrt{\varepsilon\mu}$, frequency $f =$ 572.6 MHz, the dielectric constant and permeability of medium are $\varepsilon = \varepsilon_0$, $\mu = \mu_0$ with ε_0, μ_0 being the dielectric constant and permeability of the vacuum, respectively. The solid line is the exact solution by the MIE series [35], where the circles ($\circ$) are the solution by the original RWG basis, the dots ($\cdot$) are by the first order method, and the plus ($+$) are by the second order method. It clearly shows the advantage of higher order methods.

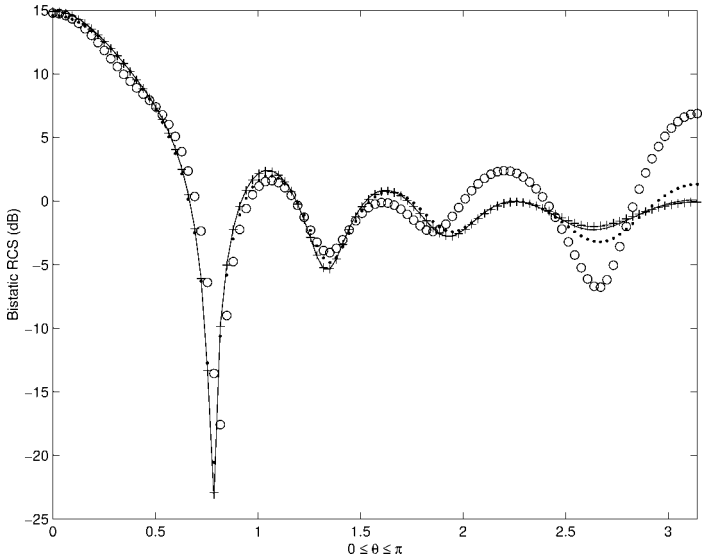

Figure 7. Bistatic RCS of a 3-D sphere (circles – RWG basis, dots – first order basis, plus – second order basis; solid line – MIE series solution).

5. Fast solver for layered media: an $O(N^{4/3}\log N)$ algorithm

In this section, we will address the fast solution of algebraic equation (13). As the number of unknowns will be large for large-scale body scattering, the direct solution of equation (13) of order $O(N^3)$ will be prohibitively expensive. Therefore, the usual practice is to apply a Krylov subspace based iteration method. A necessary step for the Krylov subspace method, such as GMRES [30], will involve the product of the matrix and a solution vector. As the matrix Z (13) is a full matrix, a direct multiplication will cost $O(N^2)$ operations. Many algorithms have been proposed to reduce this cost to order of $O(N\log N)$ or $O(N)$, among them the most popular one is the FMM in the case of homogeneous media. When the media is layered, the problem become more complicated. We will propose a new method to reduce this cost to $O(N^{4/3}\log N)$ for layered media.

Let us assume that we have a cluster of current sources $J(\mathbf{r}'_\beta)$ located at $\mathbf{r}'_\beta = (x'_m, y'_n, z'_l)$, $\beta = (m,n,l)$, $(m,n) \in \Delta'_l$ in nth layer and a cluster of field points $\mathbf{r}_\alpha = (x_i, y_j, z_k)$, $\alpha = (i,j,k)$, $(i,j) \in \Delta_k$ in mth layer. Δ_l is the index set for (m,n) at plane $z = z'_l$ while Δ_k is the index set for (i,j) at plane $z = z_k$. We will make the following assumption:

$$\begin{aligned} \left|\Delta'_l\right| &= O(N_x N_y), \quad 1 \leqslant l \leqslant O(N_z), \\ |\Delta_k| &= O(N_x N_y), \quad 1 \leqslant k \leqslant O(N_z). \end{aligned}$$

So the total number of source and field points are of the order $O(N_x N_y N_z)$, respectively. For simplicity of argument, let a field quantity $\phi(\mathbf{r}_\alpha)$ at $\mathbf{r}_\alpha$ be expressed as follows

$$\phi(\mathbf{r}_\alpha) = \sum_\beta \mathbf{G}\big(\mathbf{r}_\alpha, \mathbf{r}'_\beta\big)\mathbf{J}\big(\mathbf{r}'_\beta\big), \tag{49}$$

where $\mathbf{G}(\mathbf{r}_\alpha, \mathbf{r}'_\beta)$ is the dyadic Green's function which denotes the field quantity at $\mathbf{r}_\alpha$ induced by a unite current source at $\mathbf{r}'_\beta$. A direct evaluation of (49) will cost $O(N^2)$, $N = N_x N_y N_z$.

In order to reduce the cost of evaluating $\phi(\mathbf{r}_\alpha)$ for all $\mathbf{r}_\alpha$, we will first use the acceleration algorithm 1 proposed in section 3.2 to obtain an approximation to the Green's function $\mathbf{G}(\mathbf{r}_\alpha, \mathbf{r}'_\beta) = \mathbf{G}(\rho; z_k, z'_l)$, $\rho = |(x_i, y_j) - (x'_m, y'_n)|$ as follows

$$\begin{aligned}\mathbf{G}\big(\rho; z, z'\big) &= \int_C \mathrm{d}k_\rho J_0(\rho k_\rho)\widetilde{\mathbf{G}}\big(k_\rho; z, z'\big)\widetilde{\psi}_a(k_\rho) \\ &= \frac{1}{2}\int_{C'} \mathrm{d}k_\rho H_0^{(1)}(\rho k_\rho)\widetilde{\mathbf{G}}\big(k_\rho; z, z'\big)\widetilde{\psi}_a(k_\rho),\end{aligned} \tag{50}$$

where C is the contour in figure 2, C' is the extension of C by a mirror image with respect to the origin, $\widetilde{\mathbf{G}}(k_\rho; z, z')$ is the spectral form for the Green's function.

Now discretizing the integral in (50) using numerical quadratures along C', we have

$$\mathbf{G}(\rho; z, z') = \frac{1}{2}\sum_{s=1}^{N_q} \omega_s H_0^{(1)}\big(\rho k_\rho^s\big)\widetilde{\mathbf{G}}\big(k_\rho^s; z, z'\big)\widetilde{\psi}_a\big(k_\rho^s\big), \tag{51}$$

where ω_s is the quadrature weights and $N_q = O(kd_{\max})$ is the number of quadrature points, here k is the wave number and $d_{\max}$ is the diameter of the scatter.

The spectral Green's function $\widetilde{G}(k_\rho; z, z')$ can be written as sums of terms involving the product of k_ρ-functions and z-functions [6]

$$\widetilde{\mathbf{G}}\big(k_\rho; z, z'\big) = \mathbf{R}(k_\rho)F\big(z, z', k_\rho\big),$$

where $\mathbf{R}(k_\rho)$ is a matrix function of k_ρ and

$$F\big(z, z', k_\rho\big) = \exp\big(\pm jk_{nz}z' \pm jk_{mz}z\big),$$

$k_{nz} = \sqrt{k_n^2 - k_\rho^2}$, $k_n^2 = \omega^2\varepsilon_n\mu_n$.

So (51) can be rewritten as

$$\mathbf{G}\big(\rho; z, z'\big) = \sum_{s=1}^{N_q} \mathbf{\Gamma}_s H_0^{(1)}\big(\rho k_\rho^s\big)F\big(z, z', k_\rho^s\big), \tag{52}$$

where $\mathbf{\Gamma}_s = \frac{1}{2}\omega_s\mathbf{R}(k_\rho^s)\widetilde{\psi}_a(k_\rho^s)$.

Now we assume that there is a common or several common index set Δ which approximates all Δ_k,

$$\Delta \sim \Delta_k, \quad 1 \leqslant k \leqslant \mathrm{O}(N_z), \qquad |\Delta| = \mathrm{O}(N_x N_y),$$

here the approximation is defined in terms of the distance in (x, y)-plane.

For each $(x_i, y_j) \in \Delta,\ 1 \leqslant k \leqslant \mathrm{O}(N_z)$

$$\begin{aligned}\phi(x_i, y_j, z_k) &= \sum_{(m,n,l)} \mathbf{G}\big(x_i, y_j, z_k; x'_m, y'_n, z'_l\big)\mathbf{J}\big(x'_m, y'_n, z'_l\big) \\ &= \sum_{s=1}^{N_q} \mathbf{\Gamma}_s \sum_l F\big(z_k, z'_l, k^s_\rho\big) \sum_{(m,n)\in\Delta_l} H_0^{(1)}\big(k^s_\rho \big|(x_i, y_j) - \big(x'_m, y'_n\big)\big|\big)\mathbf{J}\big(x'_m, y'_n, z'_l\big) \\ &= \sum_{s=1}^{N_q} \mathbf{\Gamma}_s \sum_l F\big(z_k, z'_l, k^s_\rho\big)\psi_s\big(x_i, y_j, z'_l\big),\end{aligned}$$

where

$$\psi_s\big(x_i, y_j, z'_l\big) = \sum_{(m,n)\in\Delta_l} H_0^{(1)}\big(k^s_\rho \big|(x_i, y_j) - \big(x'_m, y'_n\big)\big|\big)\mathbf{J}\big(x'_m, y'_n, z'_l\big). \tag{53}$$

We will implement the sum of (49) in following two steps:

- **Step 1.** Evaluate all $\psi_s(x_i, y_j, z'_l),\ (i, j) \in \Delta,\ 1 \leqslant l \leqslant \mathrm{O}(N_z),\ 1 \leqslant s \leqslant N_q$.
  For each z'_l, the cost to evaluate $\psi_s(x_i, y_j, z'_l)$ of (53) for all $(i, j) \in \Delta$ is of order $\mathrm{O}(N_x N_y \log(N_x N_y))$ by the two-dimensional multilevel Fast Multipole Method. Therefore, we have
  $$\text{Subtotal cost} = \mathrm{O}\big(N_q N_z N_x N_y \log(N_x N_y)\big).$$
- **Step 2.** Evaluate all $\phi(x_i, y_j, z_k), (x_i, y_j) \in \Delta,\ 1 \leqslant k \leqslant \mathrm{O}(N_z)$.
  For each (x_i, y_j), using the special format of $F(z, z', k_\rho)$, we have
  $$\begin{pmatrix} \phi(\cdot, z_1) \\ \vdots \\ \phi(\cdot, z_k) \\ \vdots \\ \phi(\cdot, z_{N_z}) \end{pmatrix} = \sum_{s=1}^{N_q} \gamma_s \begin{pmatrix} \exp(\pm jk_{mz}z_1) \\ \vdots \\ \exp(\pm jk_{mz}z_k) \\ \vdots \\ \exp(\pm jk_{mz}z_{N_z}) \end{pmatrix} \cdot \begin{pmatrix} \exp\big(\pm jk_{nz}z'_1\big) \\ \vdots \\ \exp\big(\pm jk_{nz}z'_l\big) \\ \vdots \\ \exp\big(\pm jk_{nz}z'_{N_z}\big) \end{pmatrix}^{\mathrm{T}} \begin{pmatrix} \psi_s\big(\cdot, z'_1\big) \\ \vdots \\ \psi_s\big(\cdot, z'_l\big) \\ \vdots \\ \psi_s\big(\cdot, z'_{N_z}\big) \end{pmatrix}$$
  for which the cost is $N_q N_z$.

  Therefore, we have
  $$\text{subtotal cost} = N_q \mathrm{O}(N_z N_x N_y).$$

Finally, $\phi(x_i, y_j, z_k), (x_i, y_j) \in \Delta_k$ can be approximated by interpolation from $\phi(x_i, y_j, z_k), (x_i, y_j) \in \Delta$, for which the cost will be of order $\mathrm{O}(N_x N_y N_z)$.

Now the combined total cost is of the order $N_q \mathrm{O}(N_x N_y N_z \log(N_x N_y))$. If we can assume that

$$N_q = \mathrm{O}(kd_{\max}) = \mathrm{O}\Big(k\sqrt{N_x^2 + N_y^2}\Big).$$

In the case we have $N_x = N_y = N_z = \sqrt[3]{N}$, N is the total number of unknown, then the total cost of our algorithm is $\mathrm{O}(N^{4/3} \log N)$.

References

[1] M.I. Aksun, A robust approach for the derivation of closed-form Green's functions, IEEE Trans. Microwave Theory Tech. 44 (May 1996) 651–658.

[2] L.S. Andersen and J.L. Volakis, Development and application of a novel class of hierarchical tangential vector finite elements for electromagnetics, IEEE Trans. Antennas Propag. 47(1) (1999).

[3] W. Cai, High order current basis functions for electromagnetic scattering of curved surfaces, J. Sci. Comput. 14(1) (1999) 73–105.

[4] W. Cai and T.J. Yu, Fast calculation of dyadic Green's functions for electromagnetic scattering in a multilayered medium, J. Comput. Phys. 165 (2000) 1–21.

[5] W. Cai, T.J. Yu, H. Wang and Y. Yu, High order mixed RWG basis functions for electromagnetic applications, IEEE Trans. Microwave Theory Tech. 49 (July 2001) 1295–1303.

[6] W.C. Chew, *Waves and Fields in Inhomogeneous Media*, 2nd ed. (IEEE Press, New York, 1995).

[7] Y.L. Chow, J.J. Yang, D.G. Fang and G.E. Howard, A closed form spatial Green's function for the thick microstrip substrate, IEEE Trans. Microwave Theory Tech. 39 (March 1991) 588–592.

[8] T.J. Cui and W.C. Chew, Fast evaluation of Sommerfeld integrals for EM scattering and radiation by three-dimensional buried objects, Research Report No. CCEM-34-97, University of Illinois, Urbana, IL (December 1997).

[9] I. Daubechies, *Ten Lectures on Wavelets*, Conference Board of the Mathematical Sciences Series, Vol. 61 (SIAM, Philadelphia, 1992).

[10] L. Demkowicz, L. Vardapetyan and W. Rachowicz, Hp-adaptive edge finite elements for Maxwell equations, in: *ACES '98*, Monterey, CA, 16–20 March 1998.

[11] L. Greengard and V. Rokhlin, A fast algorithm for particle simulation, J. Comput. Phys. 73 (1987) 325–348.

[12] R.F. Harrington, *Time Harmonic Electromagnetic Fields* (McGraw-Hill, New York, 1961).

[13] R.F. Harrington, *Field Computation by Moment Methods* (Macmillian, New York, 1968).

[14] R.F. Harrington, Characteristic modes for antennas and scatters, in: *Numerical and Asymptotic Techniques in Electromagnetics*, ed. R. Mittra, Topics in Applied Physics, Vol. 3 (Springer, Berlin, 1975).

[15] B. Hu and W.C. Chew, Fast inhomogeneous plane wave algorithm for electromagnetic solution in layered medium structures: two-dimensional case, Radio Sci. 35(1) (2000) 31–43.

[16] D. Kopriva, S.L. Woodruff and M.Y. Hussaini, Discontinuous spectral elment approximation of Maxwell's equation, in: *Proc. of the Internat. Symposium on Discontinuous Galerkin Methods*, eds. B. Cockburn, G. Karniadakis and C.-W. Shu (Springer, New York, 2000).

[17] E. Kreyszig, *Differential Geometry* (Dover, New York, 1991).

[18] K. Michalski and J.R. Mosig, Multilayered media Green's functions in the integral equation formulations, IEEE Trans. Antennas Propag. 35(11) (1987) 1299–1301.

[19] E. Michielssen and W.C. Chew, The fast steepest descent path algorithm for analyzing scattering from two dimensional objects, Radio Sci. 31(5) (1996) 1215–1224.

[20] J.R. Mosig, Integral equation technique, in: *Numerical Techniques for Microwave and Millimeter-Wave Passive Structure*, ed. T. Itoh (Wiley, New York, 1989) pp. 133–213.

[21] C. Muller, *Foundation of the Mathematical Theory of Electromagnetic Waves* (Springer, Berlin, 1969).

[22] K. Nabors and J. White, Fastcap: A multipole accelerated 3-D capacitance extraction program, IEEE Trans. Comput.-Aided Design Integrated Circuits Systems 10 (1991) 1447–1459.
[23] J.C. Nedelec, Computation of Eddy current on a surface in R^3 by finite element methods, SIAM J. Numer. Anal. 15(3) (1978) 580–594.
[24] Y.C. Pan and W.C. Chew, A hierachical fast multipole method for strated media, Microwave Optic. Technol. Lett. 27(1) (2000).
[25] B.D. Popovic and B.M. Kolundzija, *Analysis of Metallic Antennas and Scatters* (IEE Press, London, 1994).
[26] P.A. Raviart and J.M. Thomas, A mixed finite element method for 2nd order elliptic problems, in: *Lecture Notes in Mathematics*, Vol. 606 (Springer, Berlin/New York, 1977) pp. 292–315.
[27] S.M. Rao, D.R. Wilton and A.W. Glisson, Electromagnetic scattering by surfaces of arbitrary shape, IEEE Trans. Antennas Propag. 30 (May 1982) 409–418.
[28] V. Rokhlin, Diagonal forms of translation operators for the Helmholtz equation in three dimensions, Appl. Comput. Harmonic Analysis 1 (1993) 82–93.
[29] V. Rokhlin, Rapid solution of integral equations of scattering theory in two dimensionals, J. Comput. Phys. 36(2) (1990) 414–439.
[30] Y. Saad and M.H. Schultz, GMRES: A generalized minimal residual algorithm for solving nonsymmetric linear system, SIAM J. Sci. Statist. Comput. 7 (1986) 856–869.
[31] M.I. Sancer, R.L. McClary and K.J. Glover, Electromagnetic computation using parametric geometry, Electromagnetics 10(1/2) (1990) 85–103.
[32] T.B. Senior and J.L. Volakis, *Approximate Boundary Conditions in Electromagnetics* (The Institute of Electrical Engineers, Bath, England, 1994).
[33] P.P. Silvester and R.L. Ferrari, *Finite Elements for Electrical Engineer* (Cambridge Univ. Press, Cambridge, 1996).
[34] J.M. Song and W.C. Chew, Moment method solutions using parametric geometry, J. Electromagnetic Waves Appl. 9(1/2) (1995) 71–83.
[35] J.A. Stratton, *Electromagnetic Theory* (McGraw-Hill, New York, 1941).
[36] B. Szabo and I. Babuska, *Finite Element Analysis* (Wiley, New York, 1991).
[37] J. Van Bladel, *Singular Electromagnetic Fields and Sources* (IEEE Press, New York, 1991).
[38] R.L. Wagner and W.C. Chew, A ray-propagation fast multipole algorithm, Microwave Optic. Technol. Lett. 7(10) (1994) 435–438.
[39] S. Wandzura, Electric current basis functions for curved surfaces, Electromagnetics 12 (1992) 77–91.
[40] T. Warburton, Application of the discontinuous Galerkin method to Maxwell equations using unstructured polymorphic hp-finite elments, in: *Proc. of the Internat. Symposium on Discontinuous Galerkin Methods*, eds. B. Cockburn, G. Karniadakis and C.-W. Shu (Springer, New York, 2000).
[41] J.P. Webb, Edge elements and what they can do for you, IEEE Trans. Magn. 29 (March 1993) 1460–1465.
[42] D.L. Wilkes and C.-C. Cha, Method of moments solution with parametric curved triangular patches, in: *1991 Internat. IEEE AP-S Symposium Digest*, London, ON, 1991, pp. 1512–1515.
[43] K.S. Yee, Numerical solution of initial boundary value problems involving Maxwell equations in isotropic media, IEEE Trans. Antennas Propag. 14 (May 1966) 302–307.
[44] T.J. Yu and W. Cai, High-order window functions and fast algorithms for calculating dyadic electromagnetic Green's functions in multilayered media, Radio Sci. 36(4) (2001) 559–570.